Environmental
Science
Water Research & Technology

ROYAL SOCIETY
OF CHEMISTRY

PAPER

View Article Online
View Journal

Check for updates

Cite this: DOI: 10.1039/d6ew00171h

Evaluating interferences in the external calibration method for hydroxyl radical scavenging capacity measurement

Fateme Mohamadi,[a] Tianyi Chen,[b] Ron Hofmann [b] and Chengjin Wang *[a]

In most advanced oxidation processes (AOPs), hydroxyl radicals (·OH) are produced to transform micropollutants. However, they can also be consumed by non-target compounds including organic and some inorganic matter, known as ·OH scavengers. The pseudo-first order consumption rate of ·OH is termed as the hydroxyl radical scavenging capacity (HRSC). HRSC directly influences AOP performance, which is a crucial parameter for AOP design and operation. An external calibration method has been developed to measure HRSC, using methylene blue (MB) as the probe compound. This method assumes that MB only reacts with ·OH, but experimental investigation is needed to confirm this. In this study, MB decay was monitored under reaction conditions featuring high concentrations of superoxide radicals, organic radicals, carbonate radicals, and singlet oxygen. The results showed that these reactive species did not contribute to MB decay. Additionally, as chloride, bromide, and chloramines may introduce new reactive species through UV photolysis or reaction with ·OH, their impacts on HRSC measurement were investigated. Our results show that chloride has no impact on HRSC, while bromide at low mg L^{-1} levels significantly increases it. Chloramines were found to significantly increase HRSC. Our findings confirm that the external calibration method is reliable for most drinking water samples due to the negligible interferences from non-·OH species. For water samples containing chloramines, a protocol was developed to measure background HRSC with chloramines quenched using sodium sulfite. This approach assumes that the contribution of chloramines can be modeled when their concentrations are accurately determined.

Received 15th February 2026,
Accepted 16th May 2026

DOI: 10.1039/d6ew00171h

rsc.li/es-water

Water impact

This study evaluated uncertainties in the external calibration method for hydroxyl radical scavenging capacity (HRSC) measurement. Methylene blue was confirmed as a suitable hydroxyl radical probe, and interferences from carbonate radicals, superoxide, and singlet oxygen were negligible. Overall, the results validate external calibration as a robust approach for HRSC monitoring and cost-effective optimization of advanced oxidation processes.

1. Introduction

Advanced oxidation processes (AOPs) generate hydroxyl radicals (·OH), which are strong oxidants reacting with numerous species in water. Although ·OH is typically used to oxidize micropollutants, it can also be scavenged by non-target compounds (*e.g.*, natural organic matter and bicarbonate).[1] This scavenging effect decreases the concentration of available ·OH to destroy the target contaminants; therefore, it is useful to determine the extent of water scavenging to guide AOP design and operation. Quantitatively, the hydroxyl radical scavenging capacity (HRSC) is the sum of the pseudo first-order consumption rates of ·OH by non-target compounds in a water sample, which is the sum of each scavenger's molar concentration $[S_i]$ (M) multiplied by its second-order reaction rate constant k_i (M^{-1} s^{-1}) in ·OH reactions (eqn (1)).

$$\mathrm{HRSC} = \sum k_i[S_i] \tag{1}$$

The HRSC of a water sample with known constituents and known hydroxyl reaction rates can be calculated with eqn (1). However, the concentration and reactivity of individual ·OH-consuming constituents in most water samples are unknown, necessitating the development of an experimental method to directly measure the HRSC. Therefore, an external calibration method was developed for HRSC measurement, which

---

[a] Department of Civil Engineering, University of Manitoba, 15 Gillson St, Winnipeg, Manitoba R3T 5V6, Canada. E-mail: chengjin.wang@umanitoba.ca; Tel: +1 204 474 8381
[b] Department of Civil and Mineral Engineering, University of Toronto, 35 St. George Street, Toronto, Ontario M5S 1A4, Canada

significantly simplified the test procedure and shortened the testing time compared to conventional methods.[2]

In the external calibration method, fixed amounts of methylene blue (MB) and H_2O_2 are added to standard solutions with known scavenging capacities. The solutions are then exposed to a fixed UV fluence, which photolyzes H_2O_2 to generate ·OH at a constant rate. The MB decay rate in each solution, which is inversely related to the solution's HRSC, is monitored using a spectrophotometer. A calibration curve relating hydroxyl radical scavenging capacity to the MB decay rate is established from these standards. Under identical UV/H_2O_2 conditions, MB decay in samples with unknown HRSC is measured and the resulting decay rates are converted to HRSC values using the calibration curve.

This method assumes that the colour loss due to MB decay is only attributed to the reaction between hydroxyl radicals and MB. However, during the UV/H_2O_2 reaction in a water sample, there are reactive species generated other than ·OH, such as carbonate radicals ($CO_3^{\bullet-}$),[3] various organic radicals,[4] superoxide radicals ($O_2^{\bullet-}$),[5] and singlet oxygen ($^1O_2$).[6] If these species react with MB, the resulting measurement is not representative of solely ·OH scavenging, and the MB decay rate would be accelerated and the measured HRSC would be falsely overestimated. Furthermore, the external calibration method has not been tested in the water reuse scenario, especially for reverse osmosis (RO) permeate containing chloramines. The RO permeate is expected to have low HRSC due to low concentrations of total organic carbon (TOC) (<0.5 mg L^{-1} as C) and inorganic carbon (<15 mg L^{-1} as $CaCO_3$),[7] but the permeate usually contains residual chloramines applied upstream for membrane fouling control.[8] Chloramines contribute to HRSC through their reactions with ·OH but they can also generate ·OH due to UV photolysis. This may introduce errors to the external calibration method by invalidating the constant ·OH generation assumption. Additionally, the impact of chloride (Cl^-) and bromide (Br^-) on HRSC measurement has not been reported. Chloride and bromide have the potential to react with ·OH and produce secondary or tertiary reactive species such as $Cl_2^{\bullet-}$, $ClOH^{\bullet-}$, $Br_2^{\bullet-}$, and $BrOH^{\bullet-}$.[9] The reactivity of these halogen-containing radicals toward MB and their impact on HRSC measurement remain unknown.

To address the uncertainties associated with the external calibration method, this study was designed to (1) test the reactivity of MB towards superoxide radicals, organic radicals, carbonate radicals, and singlet oxygen under conditions featuring high concentrations of each of these reactive species, (2) measure the HRSC of synthetic RO samples with and without quenching chloramines, and (3) compare the impact of chloride and bromide on the ·OH scavenging capacity measurement.

2. Materials and methods

2.1 Chemicals and materials

All chemicals used in this study were ACS grade unless otherwise specified. Methylene blue hydrate powder (92%) and hydrogen peroxide (30% w/w) were purchased from Sigma-Aldrich and used to prepare 1 g L^{-1} MB stock solution and 10 g L^{-1} H_2O_2 stock solution, respectively. Isopropyl alcohol, furfuryl alcohol, benzoic acid, nitrobenzene, sodium sulfite, sodium carbonate, and sodium bisulfite were also sourced from Sigma-Aldrich. Acetone (NF FCC grade), phenol, methanol (HPLC grade), ethanol and acetic acid were purchased from Fisher Scientific. Acetonitrile was purchased from VWR Chemicals BDH. Humic acid derived from the Suwannee River was obtained from the International Humic Substances Society.

A synthetic water matrix was prepared by diluting Winnipeg's tap water 15-fold with Milli-Q water, resulting in a final TOC ≤ 0.3 mg C per L and pH close to neutral. The free chlorine concentration was always negligible before tests. This matrix was used for all test conditions except the bromide and chloride effect tests, for which tap water was used directly (TOC: 4.3 mg C per L, Cl^-: ~5 mg L^{-1}, Br^-: <0.05 mg L^{-1}, residual free chlorine: negligible before tests as it was quenched by H_2O_2), and the singlet oxygen effect tests, for which Milli-Q water was used. When needed, pH was adjusted using HCl or NaOH solutions. To avoid buffer interference with HRSC measurements, no buffer was used for pH adjustment. The solution pH remained stable for several minutes, sufficient to complete the HRSC measurement. The pH was monitored before and after the HRSC measurement to confirm its short-term stability, remaining within ±0.2 units. The primary reason for preparing the synthetic water using diluted Winnipeg water was to simulate the TOC level in the RO permeate for studying the effect of chloramines on HRSC measurement, although it was also used in most of the other experiments.

2.2 Generation of non-·OH species

2.2.1 Carbonate radical ($CO_3^{\bullet-}$). To produce carbonate radicals ($CO_3^{\bullet-}$), 20 mM of sodium carbonate (2.2 g L^{-1}) was added to the 40 mL synthetic water sample in the presence of 1.47 mM (50 mg L^{-1}) hydrogen peroxide and 5 μM MB, resulting in a pH of 11 ± 0.05. The HRSC of carbonate at this pH would be around 6.2×10^6 s^{-1} (at an average pH of 10.9, approximately 80% of the added inorganic carbon is present as carbonate, and the product of carbonate concentration and the rate constant $k = 3.9 \times 10^8$ M^{-1} s^{-1} (ref. 10) is 6.2×10^6 s^{-1}, neglecting the contribution from bicarbonate), more than 50 times higher than the combined HRSC caused by the TOC, the spiked MB, and the H_2O_2, which was approximately 1.0×10^5 s^{-1} as estimated based on their concentrations and reactivities toward ·OH. Being exposed to UV light generated using a collimated beam system (Fig. S1), almost all the generated hydroxyl radicals were converted into $CO_3^{\bullet-}$ resulting in a high concentration of $CO_3^{\bullet-}$ and a very low amount of hydroxyl radicals. Under these conditions, if the decay rate of methylene blue was negligible, it would indicate the negligible contribution of carbonate radicals to methylene blue degradation.

2.2.2 Organic radicals. Similarly, methylene blue decay was monitored under conditions when organic radicals were the dominant reactive species in synthetic water samples. Such conditions were achieved by applying organic compounds at concentrations high enough to convert almost all the hydroxyl radicals into organic radicals. The organic compounds tested in this study ranged from simple structure molecules (*e.g.*, ethanol) to complex molecules (*e.g.*, humic acids) with different functional groups (*e.g.*, hydroxyl, carboxylate, and nitrile) and reactivities to investigate various organic radicals which might be present in the UV/H_2O_2 process, including carbon centered radicals such as methyl radicals, oxygen-centered radicals such as alkoxy radicals, and others. The tested organic compounds and their concentrations are listed in Table 1, along with their contribution to HRSC. As shown in Table 1, the spiked organic matter exhibited sufficient HRSC to consume nearly all of the hydroxyl radicals and generate various organic radicals. Each compound's impact on MB decay was evaluated individually in the presence of 50 mg L^{-1} H_2O_2 and 5 μM methylene blue (MB). Furthermore, a solution of 150 mg C per L (approximately 13 mM as C) humic acid from Suwannee River from the International Humic Substances Society was prepared to be tested as a representation of natural organic matter (NOM).

2.2.3 Superoxide radical ($O_2^{\bullet-}$). Another common radical in UV/H_2O_2 is superoxide ($O_2^{\bullet-}$). Hydrogen peroxide is a generator of ·OH under UV exposure, and at the same time, it also consumes ·OH as described in eqn (2) and (3). When the HRSC caused by hydrogen peroxide is higher than any other species in the water matrix, ·OH is mainly consumed by H_2O_2 and generates superoxide radicals. This means that at high concentrations of hydrogen peroxide, superoxide radicals can be dominant.[10]

$$\cdot OH + H_2O_2 \rightarrow HO_2^{\bullet} + H_2O \quad k = 2.7 \times 10^{7}\ M^{-1}\ s^{-1} \tag{2}$$

$$HO_2^{\bullet} \leftrightarrow O_2^{\bullet-} + H^{+} \quad pK_a = 4.7 \tag{3}$$

To investigate the contribution of superoxide radicals towards MB decay, benzoic acid (BA) and nitrobenzene (NB), along with MB, were applied to synthetic water as ·OH probe compounds. While NB and BA are reported to be reactive towards hydroxyl radicals, they have no reactivity towards superoxide radicals.[14] The degradation of BA, NB, and MB, all with an initial concentration of 5 μM, was monitored at different H_2O_2 concentrations under UV as described below. The first-order decay rates of MB, BA, and NB were calculated as k'_{MB}, k'_{BA}, and k'_{NB}. If the ratio of k_{MB}/k_{BA} or k_{MB}/k_{NB} was constant at different concentrations of hydrogen peroxide, it means that the hydroxyl radical is the only contributor to MB decay as shown in eqn (4) (using BA as an example):

$$\frac{k'_{MB}}{k'_{BA}} = \frac{k_{MB}[\cdot OH]_{ss}}{k_{BA}[\cdot OH]_{ss}} = \frac{k_{MB}}{k_{BA}} \tag{4}$$

where, $[^{\bullet}OH]_{ss}$ is the steady-state concentration of the hydroxyl radical, and k_{MB} and k_{BA} are the second-order rate constants for oxidation reactions by ·OH. However, if $O_2^{\bullet-}$ contributes to MB decay, $\frac{k'_{MB}}{k'_{BA}}\left(\text{or } \frac{k'_{MB}}{k'_{NB}}\right)$ will depend on the hydrogen peroxide concentration, indicating that $O_2^{\bullet-}$ contribution is not negligible. In other words, if superoxide significantly reacts with MB, then $\frac{k'_{MB}}{k'_{BA}}$ will increase with the increase in the H_2O_2 concentration, as shown in eqn (5) (using BA as an example):

$$\frac{k'_{MB}}{k'_{BA}} = \frac{k_{MB}[\cdot OH]_{ss} + k_{MB/O_2^{\bullet-}}[O_2^{\bullet-}]_{ss}}{k_{BA}[\cdot OH]_{ss}} \tag{5}$$

where, $[O_2^{\bullet-}]_{ss}$ is the steady-state concentration of the superoxide radical, which increases with the H_2O_2 concentration, and $k_{MB/O_2^{\bullet-}}$ is the second-order rate constant for the reaction between MB and $O_2^{\bullet-}$. Therefore, by using a wide range of H_2O_2 concentrations (from 10 mg L^{-1} to 2000 mg L^{-1}), different concentrations of $O_2^{\bullet-}$ can be generated, at which the degradation of MB, BA, and NB was monitored.

2.2.4 Singlet oxygen ($^1O_2$). To generate singlet oxygen, hydrogen peroxide and sodium hypochlorite were added to Milli-Q water to produce singlet oxygen (eqn (6)),[15] and the Milli-Q water matrix was used to minimize background consumption of $^1O_2$.

$$OCl^{-} + H_2O_2 \rightarrow H_2O + Cl^{-} + {}^1O_2 \tag{6}$$

To confirm the presence of singlet oxygen at sufficient concentrations for micropollutant degradation, furfuryl alcohol (FFA), a known probe for singlet oxygen, was used.[16] Experiments were conducted by adding hydrogen peroxide

Table 1 Expected HRSC caused by tested organic species

Organic compound	Hydroxyl rate constant (M^{-1} s^{-1})	Molar concentration (M)	Expected HRSC (s^{-1})
Isopropyl alcohol (IPA)	1.9×10^{9} (ref. 11)	0.65	1.9×10^{9}
Methanol	9.0×10^{8} (ref. 11)	0.70	6.8×10^{8}
Phenol	6.0×10^{9} (ref. 11)	0.11	6.5×10^{8}
Acetate	8.5×10^{7} (ref. 12)	0.10	6.8×10^{7}
Acetonitrile	2.0×10^{7} (ref. 11)	0.25	1.1×10^{7}
Ethanol	1.9×10^{9} (ref. 11)	0.01	2.0×10^{7}
Acetone	1.0×10^{8} (ref. 11)	0.80	8.6×10^{7}
Humic acid	3.0×10^{8} (ref. 13)	~0.013 (as C)	4.0×10^{6}

and sodium hypochlorite at a 1 : 1 molar ratio to a solution containing approximately 5 μM FFA. The decay of FFA was monitored to confirm the generation of $^1O_2$. Reaction conditions were varied with OCl^- and H_2O_2 concentrations of 1, 2, and 3 mM at room temperature. Reactions were carried out in batch glass reactors containing 100 mL of deionized water, equipped with a magnetic stirrer. The duration of each treatment was 5 min, and samples were collected immediately after that for FFA analysis as described later.

2.3 Investigating chloride and bromide impact

To investigate the effect of chloride on HRSC, sodium chloride (NaCl) was added to the tap water samples to create concentration ranges from 0 mg L^{-1} to 200 mg L^{-1} as Cl^-. Similarly, the effect of bromide was tested on HRSC measurement by adding potassium bromide (KBr) to create different concentrations of Br^- from 0 mg L^{-1} to 2 mg L^{-1}. The HRSC of each sample was measured and compared with the scavenging capacity of the water matrix before the halide ion addition.

2.4 Impact of chloramines

The impact of chloramines on HRSC measurement was investigated by adding different concentrations of chloramines (0 to 12 mg L^{-1} as Cl_2) to the synthetic water with pH adjusted to 5.5 using HCl solution (*i.e.* simulated RO). The samples were then subjected to HRSC analysis using the same method as described above. We then explored methods to quench chloramines prior to HRSC measurement, using sulfite and bisulfite as quenching agents. This was done to determine whether the quenching process could restore the HRSC to baseline values observed before chloramine addition. The quenching process is usually necessary when water samples are shipped to off-site laboratories for baseline HRSC analysis. Additional details on chloramine quenching are provided in the SI and Fig. S2.

2.5 Analytical methods

The pH was measured using an Orion Star A211 benchtop pH meter (Thermo Scientific, Waltham, Massachusetts, USA), and the TOC was analyzed using a TOC-$L_{CPH/CPN}$ analyzer (Shimadzu Corporation, Kyoto, Japan). The decay of methylene blue was monitored using a VWR V-1200 spectrophotometer (Radnor, Pennsylvania, USA) at MB's signature wavelength of 664 nm. The pseudo-first-order decay rate of MB was calculated based on the change in absorbance (A) over time. H_2O_2 concentrations were determined using the triiodide method, which is based on a reaction between H_2O_2 and potassium iodide (KI) in the presence of ammonium molybdate as a catalyst in a buffered solution.[17] The DPD colorimetric method was used to measure free and total chlorine in water samples.[18] Concentrations of nitrobenzene, benzoic acid and furfuryl alcohol were determined using an Alliance high-performance liquid chromatography (HPLC)-UV system equipped with a 2998 photodiode array (PDA) UV detector (Waters Corporation, Milford, Massachusetts, USA). A Symmetry® C_{18} reversed-phase column (3.5 μm particle size, 4.6 × 150 mm; Waters Corporation, Milford, Massachusetts, USA) was used for separation. The mobile phase comprised A (methanol) and B (10% methanol in water, pH 4 adjusted using phosphoric acid). Gradient elution ran from 30% A/70% B to 70% A/30% B and returned to 30% A/70% B. The peaks associated with the compounds were monitored at 230 nm.

Statistical analysis was performed to investigate the significance of differences in MB decay rates between direct photolysis and conditions in the presence of other radicals. The degradation rate of MB (k) under each condition was determined from the slope of the corresponding decay curve. Statistical comparisons of the k values were performed between each experimental condition and the control condition (*i.e.* MB direct photolysis). Two-tailed unpaired Student's t-test with unequal variances was applied using Microsoft Excel. Differences were considered statistically significant at $p < 0.05$.

3. Results and discussion

3.1 Reactivities of non-·OH species with MB

The potential interference of carbonate radicals, organic radicals, superoxide radicals, and singlet oxygen was evaluated to determine their contributions to MB decay. As detailed in the following sections, none of the tested radicals exhibited any reaction with MB.

3.1.1 Carbonate radical. Fig. 1 shows that the decay of MB in the presence of high concentrations of carbonate radicals —generated by quenching hydroxyl radicals with excess carbonate—is identical to that observed during MB direct photolysis (*i.e.*, no radical formation), as confirmed by the statistical analysis in Table S1. For comparison, the figure also includes the MB decay profile under typical UV/H_2O_2 conditions without elevated carbonate levels, which displays

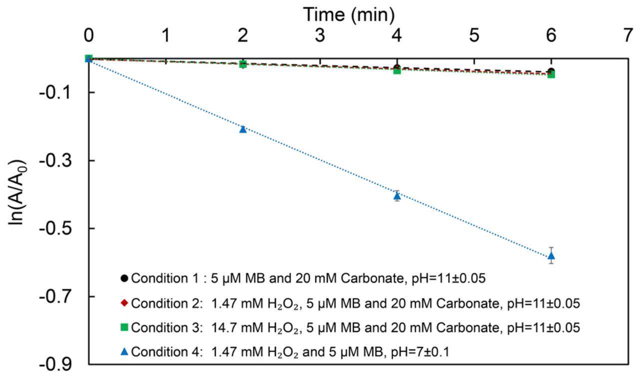

Fig. 1 Absorbance decrease in 5 μM MB at 664 nm under direct photolysis (condition 1), in the presence of carbonate radicals (conditions 2 and 3) and hydroxyl radicals (condition 4). Tests were conducted in synthetic water with an initial TOC < 0.3 mg C per L at room temperature. All tests were in triplicate, and error bars show the standard deviation.

a substantially faster decay rate. This shows negligible contribution of carbonate radicals to the MB decay rate under the conditions relevant to HRSC measurement (*e.g.*, few minutes of reaction time, tens of mg L^{-1} of H_2O_2 under a low-pressure mercury UV lamp). Notably, MB decay remained negligible when the H_2O_2 concentration was increased tenfold to 14.7 mM (500 mg L^{-1}), a condition expected to generate much higher concentrations of carbonate radicals in the presence of excess carbonate. This can be explained by the selective nature of $CO_3^{\bullet-}$ as an oxidant, targeting mainly electron-rich species such as those with N-heterocycles, reductive sulfur species, phenols, and anilines.[19] Although $k_{CO_3^{\bullet-}}$ values, the second order rate constants for carbonate radical reactions, as high as 10^8–10^9 M^{-1} s^{-1} have been reported for some anilines (*e.g.* *N*-ethyl-aniline), MB is expected to exhibit much lower rate constants because the lone pair on its nitrogen is delocalized over an extended aromatic π-system, leaving no localized electron-rich moieties available for rapid electron transfer to $CO_3^{\bullet-}$. However, a detailed mechanistic study is needed to explain the low reactivity, if any, between MB and carbonate radicals.

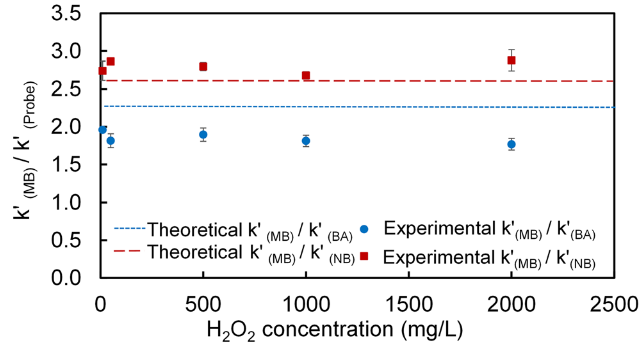

Fig. 3 Ratios of the methylene blue (MB) decay rate to benzoic acid (BA) and nitrobenzene (NB) decay rate under UV exposure at different H_2O_2 doses. All tests were conducted in synthetic water at room temperature. pH = 7 ± 0.2; $[MB]_0$ = $[NB]_0$ = $[BA]_0$ = 5 μM. The theoretical *k*′ (MB)/*k*′ (probe), excluding contribution from superoxide radicals, was calculated using rate constants reported for ·OH with MB (1.0×10^{10} M^{-1} s^{-1}),[22] NB (3.9×10^9 M^{-1} s^{-1})[11] and BA (4.3×10^9 M^{-1} s^{-1}),[11] respectively. The error bars indicate the maximum and minimum values from duplicate tests.

3.1.2 Organic radicals. Fig. 2 shows the decay of MB under UV/H_2O_2 in the presence of various organic radicals, compared with MB decay during direct photolysis (*i.e.*, no H_2O_2 and no spiked organic scavengers) and with UV/H_2O_2 treatment conducted without adding excessive organic scavengers. Under all conditions involving organic radicals, the MB decay rate was the same as or very close to its decay rate under direct photolysis (see Table S2 for statistical analysis results), significantly lower than MB decay in the presence of ·OH when no organic compound was spiked (see the line with the steep slope in Fig. 2). This indicates that the organic radicals generated from the reaction between hydroxyl radicals and various organic compounds exhibited no measurable reactivity toward MB, confirming that the tested organic radicals do not interfere with HRSC measurements when MB is used as the probe compound. This is not surprising, as most organic radicals—such as alkyl and alkoxyl radicals—have much lower redox potentials than hydroxyl radicals. Most organic radicals tend to react with oxygen to form less reactive peroxyl radicals or decompose into smaller organic species through self-decay or bimolecular reactions, rather than oxidizing MB.[20]

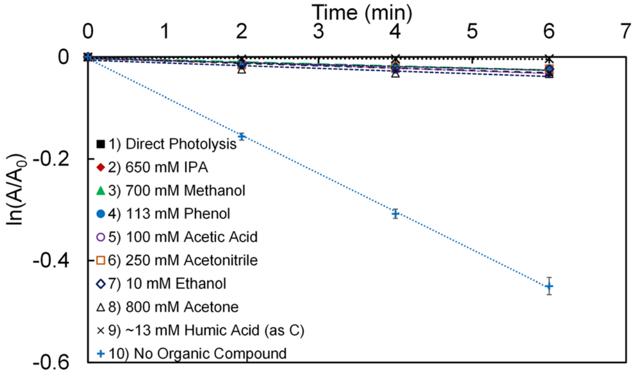

Fig. 2 Absorbance decrease in 5 μM MB at 664 nm in the presence of various organic radicals. $[H_2O_2]_0$ = 1.47 mM except for direct photolysis, and pH = 7 ± 0.2. Tests were conducted in synthetic water with an initial TOC < 0.3 mg C per L at room temperature. All tests were in triplicate, and error bars show the standard deviation. The parent compounds for the organic radicals are shown in the legend.

3.1.3 Superoxide radical. The decay of MB, BA, and NB was monitored under UV/H_2O_2 at different H_2O_2 doses, and their first-order rate constants were calculated and compared (Fig. 3). Specifically, the ratios of the MB decay rate (k'_{MB}) over the NB decay rate (k'_{NB}) at different H_2O_2 concentrations (*i.e.*, different superoxide concentrations) are plotted, along with the ratios of the MB decay rate over the BA decay rate (k'_{BA}). Fig. 3 shows that the two ratios remained consistent across a wide range of hydrogen peroxide concentrations (from 10 to 2000 mg L^{-1}). This indicates that the superoxide radical does not react with MB at a detectable rate and thus does not interfere with HRSC measurements. This is consistent with

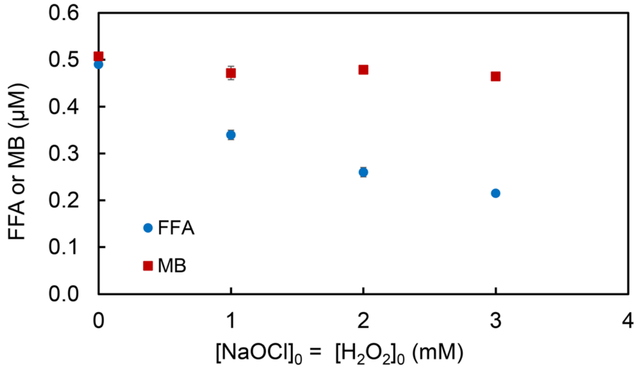

Fig. 4 Degradation of furfuryl alcohol (FFA) and methylene blue (MB) in Milli-Q water after the addition of NaOCl and H_2O_2 with a 1 : 1 molar ratio to generate singlet oxygen at room temperature and pH = 7.4 ± 0.1. The error bars indicate the maximum and minimum values from duplicate tests.

many previous studies showing the superoxide radical as a weak oxidant with negligible contributions in AOPs.[5,21]

3.1.4 Singlet oxygen. Fig. 4 illustrates the degradation of furfuryl alcohol (FFA) after adding free chlorine and hydrogen peroxide at various equimolar concentrations. When 1 mM of free chlorine and 1 mM of hydrogen peroxide were added, the concentration of FFA decreased from 0.49 μM to 0.34 μM, accounting for 31% removal. This removal was increased to 55% when the concentrations of chlorine and peroxide were tripled. As FFA is a commonly used probe for singlet oxygen, the results confirmed the effective generation of singlet oxygen through the reaction between chlorine and peroxide.[23] Fig. 4 also shows the decay of MB in the presence of singlet oxygen under the same conditions, except that FFA was replaced with MB. The negligible change in MB concentration before and after singlet oxygen generation, as indicated by the absorbance at 664 nm, confirms that singlet oxygen does not contribute to MB degradation fast enough even in the efficient singlet oxygen generating system (*i.e.*, the classical chlorine–peroxide mixture). Considering that singlet oxygen generation in the UV/H_2O_2 system occurs *via* secondary reactions and is less efficient than that in the NaOCl/H_2O_2 system, we further postulate that singlet oxygen's contribution to MB decay in the HRSC measurements is negligible.

3.2 Effect of chloride and bromide on ·OH scavenging capacity measurement

The addition of chloride to tap water samples at doses up to 200 mg L^{-1} had no significant impact on scavenging capacity, which remained close to that before chloride spiking (Fig. 5a). This is consistent with previous findings that chloride has limited impact on the UV/H_2O_2 process.[24] Although chloride reacts fast with hydroxyl radicals (eqn (7)), the reverse reaction is also fast at pH levels relevant to water treatment (eqn (8)), generating the ·OH back through instant disintegration of the product from eqn (7). The net result is the negligible HRSC from chloride.[25,26] The contribution of chlorine radicals is not relevant here. Once $ClOH^{\bullet-}$ is formed, further generation of chlorine radicals requires its protonation to form $ClOH_2^{\bullet}$. This intermediate can then lose H_2O to produce $Cl^{\bullet}$. However, this pathway requires a pH below 4.[26,27]

$$\cdot OH + Cl^- \rightarrow ClOH^{\bullet-} \quad k = 4.3 \times 10^9\ M^{-1}\ s^{-1} \tag{7}$$

$$ClOH^{\bullet-} \rightarrow \cdot OH + Cl^- \quad k = 6.1 \times 10^9\ s^{-1} \tag{8}$$

Different concentrations of bromide were added to tap water samples to investigate its effect on measuring HRSC. The results showed a significant influence of bromide at mg L^{-1} levels on the HRSC of water samples (Fig. 5b), with a 5.4 × 10^4 s^{-1} HRSC increase for each mg L^{-1} Br^- concentration increase. By eqn (1) with bromide's reaction rate constant with ·OH of 1.1×10^{10} M^{-1} s^{-1},[25] the theoretical HRSC of 1 mg L^{-1} of bromide was calculated to be 1.4×10^5 s^{-1}, which is higher than the experimentally observed value of 5.4×10^4 s^{-1}. This can be attributed to the reversible reaction shown in eqn (9), in which $BrOH^{\bullet-}$ rapidly dissociates to regenerate ·OH. Meanwhile, $BrOH^{\bullet-}$ can react with Br^- to form $Br_2^{\bullet-}$ (eqn (10)) or go through proton-assisted dissociation (eqn (11)) to generate $Br^{\bullet-}$, followed by conversion into $Br_2^{\bullet-}$ through eqn (12). Both $Br^{\bullet-}$ and $Br_2^{\bullet-}$ are highly selective radicals that primarily react with electron-rich species.[28] Therefore, converting hydroxyl radicals into less reactive bromine radicals increases HRSC and compromises AOP performance, as reported by Zhang and Parker.[29] Although most natural water bromide concentrations do not exceed 0.5 mg L^{-1},[30] some surface waters in Israel and Australia were reported to have concentrations up to 2–4 mg L^{-1},[31,32] making bromide a major ·OH scavenger.[25,33,34]

$$HO\cdot + Br^- \rightleftharpoons BrOH^{\bullet-} \quad k_{for} = 1.1 \times 10^{10}\ M^{-1}\ s^{-1},\ k_{rev} = 3.3 \times 10^7\ s^{-1} \tag{9}$$

$$BrOH^{\bullet-} + Br^- \rightleftharpoons Br_2^{\bullet-} + OH^- \quad k_{for} = 1.9 \times 10^8\ M^{-1}\ s^{-1},\ k_{rev} = 2.7 \times 10^6\ M^{-1}\ s^{-1} \tag{10}$$

$$BrOH^{\bullet-} + H^+ \rightleftharpoons Br\cdot + H_2O \quad k_{for} = 4.4 \times 10^{10}\ M^{-1}\ s^{-1},\ k_{rev} = 1.4 \times 10^7\ M^{-1}\ s^{-1} \tag{11}$$

$$Br\cdot + Br^- \rightleftharpoons Br_2^{\bullet-} \quad k_{for} = 1.0 \times 10^{10}\ M^{-1}\ s^{-1},\ k_{rev} = 1.0 \times 10^5\ s^{-1} \tag{12}$$

Another potential interference of bromide on HRSC measurement is the catalytic decay of H_2O_2 by bromide.[35] If

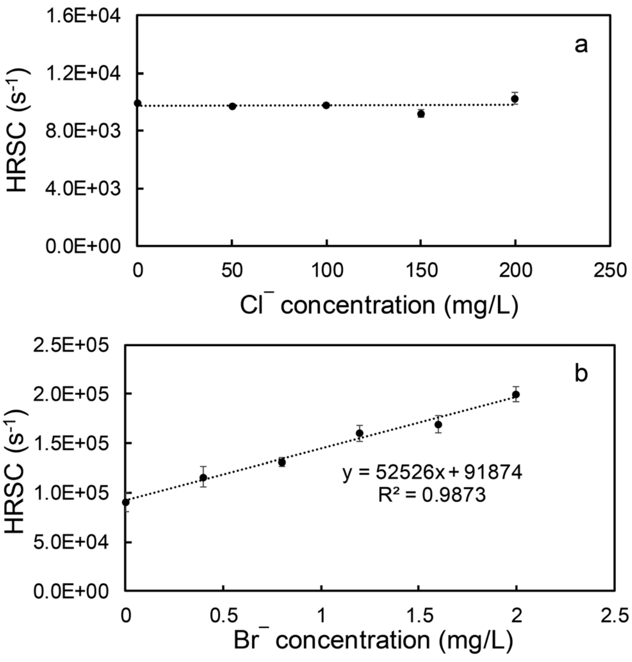

Fig. 5 HRSC of tap water in the presence of a) chloride and b) bromide (TOC = 4.3 mg C per L, pH = 7.1) at room temperature. The error bars indicate the maximum and minimum values from duplicate tests.

H_2O_2 decay is significantly accelerated by the presence of bromide, the assumption of constant ·OH production in the external calibration method would be invalid. Under our test conditions, we found that such a catalytic effect on H_2O_2 decay is negligible as shown in Fig. S3, which shows similar decay rates of H_2O_2 with and without bromine over the six minutes of test time.

3.3 Effect of chloramines on the scavenging capacity measurement

HRSC measurement is complicated by the presence of chloramines in water samples, such as RO permeates in water reuse where residues of chloramines added upstream for membrane fouling control is present. Although the scavenging capacity of chloramines can be combined with the intrinsic scavenging capacity of the original water samples and measured as a single total value, the interpretation of this total may be confounded by the additional ·OH generated through chloramine photolysis. This extra radical production violates the key assumption of the external calibration method—the hydroxyl radical generation rate remains constant. Fig. 6 demonstrates the effect of chloramines on the HRSC in simulated RO, which has an initial HRSC of 1.1×10^4 s^{-1}. By adding chloramines at 2–4 mg Cl_2 per L, which were a mixture of monochloramine and dichloramine (Fig. S4), to the water matrix, the scavenging capacity increased to about 4 to 8 × 10^4 s^{-1}. When the chloramine concentration exceeded 5 mg Cl_2 per L, the HRSC showed a diminishing increase, probably because of the generation of ·OH by chloramine photolysis which compensates for the consumption of ·OH. Therefore, the true scavenging capacity caused by chloramines, which, by definition, is only determined by the chloramines' concentrations and reactivities toward hydroxyl radicals, should be higher than that measured by the external calibration method (Fig. 6). Another challenge in measuring the HRSC of chloramine-containing water is the instability of chloramines. Their concentration and speciation can change during UV-AOPs, sample shipping, and storage, which leads to uncertainties of experimentally measured HRSCs and their relevance to process optimization. Therefore, it is advisable to quench chloramines prior to HRSC measurement so that the measured HRSC represents the background value ($HRSC_b$). The HRSC by chloramines ($HRSC_c$) can then be calculated or modelled from their concentrations and corresponding rate constants. The total HRSC ($HRSC_t$) is thus the sum of $HRSC_b$ and $HRSC_c$ (eqn (13)).

$$HRSC_t = HRSC_b + HRSC_c \qquad (13)$$

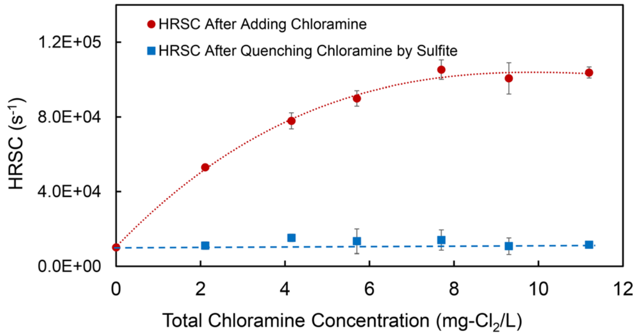

Fig. 6 HRSC before and after quenching chloramine using sodium sulfite in simulated RO at room temperature (TOC < 0.3 mg C per L; the initial pH was 5.5, and after chloramine quenching, it increased to 5.8–5.9). The error bars indicate the maximum and minimum values from duplicate tests.

Therefore, common chloramine quenching agents, sulfite/bisulfite, were tested for their suitability for such purpose. As shown in Fig. 6, when sulfite was added to water samples to stoichiometrically quench chloramines at a sulfite/Cl molar ratio of 1 : 1, the HRSC of the water samples was restored to approximately $(1.3 \pm 0.2) \times 10^4$ s^{-1}, which is close to its level before adding chloramines ($(1.1 \pm 0.2) \times 10^4$ s^{-1}). This indicates that sulfite is an effective chloramine quenching agent without changing the original HRSC of the water samples. This is because the products of the quenching reaction, ammonium and chloride, have negligible HRSC under these conditions due to their low concentrations and low reactivity towards ·OH.[26,36]

Sodium bisulfite is as effective as sodium sulfite in quenching chloramines and restoring the HRSC to the levels before the addition of chloramine, as seen in Fig. S5. However, sodium sulfite is preferred over sodium bisulfite, because sodium bisulfite decreases the water pH, for example, from an initial pH of 5.5 to 3.8 at a dose of 5.8 mg L^{-1} of $NaHSO_3$. This unusually low pH may alter the molecular structure of MB and even its reactivity toward ·OH, as implied by the slightly higher MB absorbance at pH 2–4 compared with near-neutral pH (Fig. S6). It is possible that such a low pH may invalidate the calibration curve, although further research is needed to investigate this. MB has a reported pK_a of ~3.8,[37] and near this pH protonation can alter its molecular structure and, consequently, its optical properties. Thus, changes in MB's optical response are expected primarily under acidic conditions, with minimal effects at higher pH.

Precise quenching of chloramines can be challenging, particularly during on-site sample collection. In such cases, excess sulfite is often preferred and sometimes unavoidable. Provided that the excess sulfite is counter-quenched by H_2O_2 prior to HRSC analysis, which may take half an hour or longer depending on concentrations and pH,[38] the sample's HRSC can be restored to its background values and measured with high reliability. However, the long-term (*e.g.*, days or weeks) effect of excess sulfite on samples' HRSC during sample shipping and storage has not been investigated.

4. Conclusion

This study investigated potential interferences in the external calibration method for measuring the HRSC of water samples. Our results indicated that carbonate radicals, superoxide radicals, organic radicals and singlet oxygen exhibited no detectable reactions towards MB within the typical HRSC measurement time, confirming that the decay of MB is solely attributable to its reaction with hydroxyl radicals and validating its suitability as a ·OH probe. Chloride showed no effect on the HRSC at concentrations up to 200 mg L^{-1}, whereas bromide at mg L^{-1} levels significantly increased the HRSC. Chloramines, an oxidant commonly present in RO permeates prior to UV-AOP treatment, can contribute substantially to the measured HRSC. However, experimentally quantifying their contribution is challenging because chloramines also generate hydroxyl radicals under UV irradiation, and their concentration is typically unstable in UV AOPs and during shipping and storage, making measurement inaccurate. Therefore, we recommend quenching chloramines stoichiometrically with sulfite. HRSC contribution by chloramines can then be calculated based on chloramine concentrations and the corresponding hydroxyl radical reaction rate constants. Overall, this work supports the robust application of the external calibration method in most drinking water systems and helps reduce uncertainty in measuring HRSC and optimizing UV-AOP operation. The feasibility of this method in other water matrices, such as wastewater with extreme pH or ionic strength levels, high metal concentrations, and high particle concentration, warrants further investigation.

Author contributions

Fateme Mohamadi: investigation, data analysis, and original draft. Tianyi Chen: review and editing, and funding acquisition. Ron Hofmann: conceptualization, funding acquisition, review and editing. Chengjin Wang: conceptualization, funding acquisition, review & editing.

Conflicts of interest

Authors declare that there are no competing financial interests or personal relationships with other people or funding organizations, which may have influenced their work.

Data availability

The data supporting this article have been included as part of the supplementary information (SI).

Supplementary information: the SI includes: (1) a schematic diagram of the collimated beam setup, (2) the method used to quench residual chloramines, (3) the effect of bromide on hydrogen peroxide decay, (4) the proportions of different chloramine species in total chlorine under the conditions of this study, (5) results on the quenching of chloramines by bisulfite, and (6) statistical analysis results used in the study. See DOI: https://doi.org/10.1039/d6ew00171h.

Acknowledgements

The authors acknowledge the financial support provided by the following funding organizations: the Water Research Foundation (Project No. 5194) and the California State Water Resources Control Board, the University Research Grants Program (URGP) at the University of Manitoba (Project No. 59860), and the New Investigator Operating Grant (Project No. 60131) sponsored by Research Manitoba. This material does not necessarily reflect the views and policies of the funders.

References

1 E. J. Rosenfeldt and K. G. Linden, The $R_{OH,UV}$ concept to characterize and the model UV/H_2O_2 process in natural waters, *Environ. Sci. Technol.*, 2007, **41**, 2548–2553.
2 C. Wang, E. Rosenfeldt, Y. Li and R. Hofmann, External standard calibration method to measure the hydroxyl radical scavenging capacity of water samples, *Environ. Sci. Technol.*, 2020, **54**, 1929–1937.
3 Y. Liu, X. He, X. Duan, Y. Fu, D. Fatta-Kassinos and D. D. Dionysiou, Significant role of UV and carbonate radical on the degradation of oxytetracycline in UV-AOPs: Kinetics and mechanism, *Water Res.*, 2016, **95**, 195–204.
4 E. Tsui, H. Wang and R. R. Knowles, Catalytic generation of alkoxy radicals from unfunctionalized alcohols, *Chem. Sci.*, 2020, **11**, 11124–11141.
5 Z. Luo, Y. Yan, R. Spinney, D. D. Dionysiou, F. A. Villamena, R. Xiao and D. Vione, Environmental implications of superoxide radicals: From natural processes to engineering applications, *Water Res.*, 2024, **261**, 122023.
6 L. A. C. Teixeira, M. T. C. Arellano, C. Marquez Sarmiento, L. Yokoyama and F. V. d. F. Araujo, Oxidation of cyanide in water by singlet oxygen generated by the reaction between hydrogen peroxide and hypochlorite, *Miner. Eng.*, 2013, **50–51**, 57–63.
7 M. Kwon, A. Royce, Y. Gong, K. P. Ishida and M. I. Stefan, UV/chlorine vs. UV/H_2O_2 for water reuse at Orange County Water District, CA: a pilot study, *Environ. Sci.: Water Res. Technol.*, 2020, **6**, 2416–2431.
8 D. L. McCurry, K. P. Ishida, G. L. Oelker and W. A. Mitch, Reverse osmosis shifts chloramine speciation causing re-formation of NDMA during potable reuse of wastewater, *Environ. Sci. Technol.*, 2017, **51**, 8589–8596.
9 Y. Li, W. Song, W. Fu, D. C. W. Tsang and X. Yang, The roles of halides in the acetaminophen degradation by UV/H_2O_2 treatment: Kinetics, mechanisms, and products analysis, *Chem. Eng. J.*, 2015, **271**, 214–222.
10 G. V. Buxton, C. L. Greenstock, W. P. Helman and A. B. Ross, Critical review of rate constants for reactions of hydrated electrons, hydrogen atoms and hydroxyl radicals (·OH/·O^-) in aqueous solution, *J. Phys. Chem. Ref. Data*, 1988, **17**, 513–886.
11 J. C. Crittenden, R. R. Trussell, D. W. Hand, K. J. Howe and G. Tchobanoglous, *MWH's water treatment: principles and design*, Wiley, New Jersey, 2012.

12 K. Sehested, J. Holcman, E. Bjergbakke and E. J. Hart, Ozone decomposition in aqueous acetate solutions, *J. Phys. Chem.*, 1987, **91**, 2359–2361.

13 N. Moore, C. Wang, S. Andrews and R. Hofmann, On the increasing competitiveness of UV/Cl to UV/H_2O_2 advanced oxidation as the organic carbon concentration increases, *Water Res.*, 2023, **242**, 120227.

14 B. Velika and I. Kron, Antioxidant properties of benzoic acid derivatives against superoxide radical, *Free Radicals Antioxid.*, 2012, **2**, 62–67.

15 J. K. Hurst, P. A. G. Carr, F. E. Hovis and R. J. Richardson, Hydrogen peroxide oxidation by chlorine compounds. Reaction dynamics and singlet oxygen formation, *Inorg. Chem.*, 1981, **20**, 2435–2438.

16 E. Appiani, R. Ossola, D. E. Latch, P. R. Erickson and K. McNeill, Aqueous singlet oxygen reaction kinetics of furfuryl alcohol: effect of temperature, pH, and salt content, *Environ. Sci.: Processes Impacts*, 2017, **19**, 507–516.

17 N. V. Klassen, D. Marchington and H. C. E. McGowan, H_2O_2 determination by the I_3^- method and by $KMnO_4$ titration, *Anal. Chem.*, 1994, **66**, 2921–2925.

18 A. D. Eaton, M. A. H. Franson, A. P. H. Association, A. W. W. Association and W. E. Federation, *Standard methods for the examination of water & wastewater*, American Public Health Association, 2005.

19 L. Wojnárovits, T. Tóth and E. Takács, Rate constants of carbonate radical anion reactions with molecules of environmental interest in aqueous solution: A review, *Sci. Total Environ.*, 2020, **717**, 137219.

20 S. Yang, S. Sun, Z. Xie, Y. Dong, P. Zhou, J. Zhang, Z. Xiong, C.-S. He, Y. Mu and B. Lai, Comprehensive insight into the common organic radicals in advanced oxidation processes for water decontamination, *Environ. Sci. Technol.*, 2024, **58**, 19571–19583.

21 L. Bai, L. He, Y. Fu, C. Chu, Z. Wei, R. Spinney, D. D. Dionysiou, Y. Liang and R. Xiao, New insight to superoxide radical-mediated degradation of pentachlorophenate: Kinetic determination and theoretical calculations, *Chem. Commun.*, 2022, **58**, 2666–2669.

22 Q. V. Vo, L. T. T. Thao, T. D. Manh, M. V. Bay, B.-T. Truong-Le, N. T. Hoa and A. Mechler, Reaction of methylene blue with OH radicals in the aqueous environment: mechanism, kinetics, products and risk assessment, *RSC Adv.*, 2024, **14**, 27265–27273.

23 W. R. Haag, J. r. Hoigne, E. Gassman and A. M. Braun, Singlet oxygen in surface waters — Part I: Furfuryl alcohol as a trapping agent, *Chemosphere*, 1984, **13**, 631–640.

24 W. Zhang, S. Zhou, J. Sun, X. Meng, J. Luo, D. Zhou and J. Crittenden, Impact of chloride ions on UV/H_2O_2 and UV/persulfate advanced oxidation processes, *Environ. Sci. Technol.*, 2018, **52**, 7380–7389.

25 J. E. Grebel, J. J. Pignatello and W. A. Mitch, Effect of halide ions and carbonates on organic contaminant degradation by hydroxyl radical-based advanced oxidation processes in saline waters, *Environ. Sci. Technol.*, 2010, **44**, 6822–6828.

26 J. Fang, Y. Fu and C. Shang, The roles of reactive species in micropollutant degradation in the UV/free chlorine system, *Environ. Sci. Technol.*, 2014, **48**, 1859–1868.

27 L. Wojnárovits and E. Takács, Rate constants of dichloride radical anion reactions with molecules of environmental interest in aqueous solution: a review, *Environ. Sci. Pollut. Res.*, 2021, **28**, 41552–41575.

28 Y. Lei, X. Lei, P. Westerhoff, X. Tong, J. Ren, Y. Zhou, S. Cheng, G. Ouyang and X. Yang, Bromine radical ($Br\cdot$ and $Br_2^{\bullet-}$) reactivity with dissolved organic matter and brominated organic byproduct formation, *Environ. Sci. Technol.*, 2022, **56**, 5189–5199.

29 K. Zhang and K. M. Parker, Halogen radical oxidants in natural and engineered aquatic systems, *Environ. Sci. Technol.*, 2018, **52**, 9579–9594.

30 World Health Organization, Bromide in drinking-water : background document for development of WHO guidelines for drinking-water quality, 2009.

31 A. Wang, Z. Hua, Z. Wu, C. Chen, S. Hou, B. Huang, Y. Wang, D. Wang, X. Li, C. Li and J. Fang, Insights into the effects of bromide at fresh water levels on the radical chemistry in the UV/peroxydisulfate process, *Water Res.*, 2021, **197**, 117042.

32 R. S. Magazinovic, B. C. Nicholson, D. E. Mulcahy and D. E. Davey, Bromide levels in natural waters: its relationship to levels of both chloride and total dissolved solids and the implications for water treatment, *Chemosphere*, 2004, **57**, 329–335.

33 I. Lampre, J.-L. Marignier, M. Mirdamadi-Esfahani, P. Pernot, P. Archirel and M. Mostafavi, Oxidation of bromide ions by hydroxyl radicals: spectral characterization of the intermediate $BrOH^{\bullet-}$, *J. Phys. Chem. A*, 2013, **117**, 877–887.

34 Y. Xue, Z. Wang, R. Naidu, R. Bush, F. Yang, J. Liu and M. Huang, Role of halide ions on organic pollutants degradation by peroxygens-based advanced oxidation processes: A critical review, *Chem. Eng. J.*, 2022, **433**, 134546.

35 W. C. Bray and R. S. Livingston, The catalytic decomposition of hydrogen peroxide in a bromine-bromide solution, and a study of the steady state, *J. Am. Chem. Soc.*, 1923, **45**, 1251–1271.

36 X. Yang, Y. Tao and J. G. Murphy, Kinetics of the oxidation of ammonia and amines with hydroxyl radicals in the aqueous phase, *Environ. Sci.: Processes Impacts*, 2021, **23**, 1906–1913.

37 J. J. Salazar-Rabago, R. Leyva-Ramos, J. Rivera-Utrilla, R. Ocampo-Perez and F. J. Cerino-Cordova, Biosorption mechanism of methylene blue from aqueous solution onto white pine (*Pinus durangensis*) sawdust: Effect of operating conditions, *Sustainable Environ. Res.*, 2017, **27**, 32–40.

38 C. Wang, M. Hofmann, A. Safari, I. Viole, S. Andrews and R. Hofmann, Chlorine is preferred over bisulfite for H_2O_2 quenching following UV-AOP drinking water treatment, *Water Res.*, 2019, **165**, 115000.